Title

Podocyte-specific soluble epoxide hydrolase deficiency in mice attenuates acute kidney injury

Journal

The FEBS Journal, 284(13)

ISSN

1742-464X

Authors

Bettaieb, Ahmed
Koike, Shinichiro
Chahed, Samah
et al.

Publication Date

2017-07-01

DOI

10.1111/febs.14100

Peer reviewed

The FEBS Journal

FEBS PRESS science publishing by scientists

EDITOR'S CHOICE

Podocyte-specific soluble epoxide hydrolase deficiency in mice attenuates acute kidney injury

Ahmed Bettaieb[1,2], Shinichiro Koike[1], Samah Chahed[1], Yi Zhao[2], Santana Bachaalany[1], Nader Hashoush[1], James Graham[1], Huma Fatima[3], Peter J. Havel[1,4], Artiom Gruzdev[5], Darryl C. Zeldin[5], Bruce D. Hammock[6,7] and Fawaz G. Haj[1,7,8]

1 Department of Nutrition, University of California Davis, CA, USA
2 Department of Nutrition, University of Tennessee-Knoxville, TN, USA
3 Department of Pathology, University of Alabama at Birmingham, AL, USA
4 Department of Molecular Biosciences, School of Veterinary Medicine, University of California Davis, CA, USA
5 Division of Intramural Research, National Institute of Environmental Health Sciences, Durham, NC, USA
6 Department of Entomology and Nematology, University of California Davis, CA, USA
7 Comprehensive Cancer Center, University of California Davis, Sacramento, CA, USA
8 Division of Endocrinology, Diabetes, and Metabolism, Department of Internal Medicine, University of California Davis, Sacramento, CA, USA

Keywords
knockout mice; podocyte; proteinuria; soluble epoxide hydrolase

Correspondence
F. G. Haj, Department of Nutrition, University of California Davis, 3135 Meyer Hall, Davis, CA 95616, USA
Fax: +1 (530) 752 8966
Tel: +1 (530) 752 3214
E-mail: fghaj@ucdavis.edu
and
A. Bettaieb, Department of Nutrition, University of Tennessee-Knoxville, Knoxville, TN 37996, USA
Fax: +1 (865) 974 8718
Tel: +1 (865) 974 6267
E-mail: abettaie@utk.edu

(Received 22 December 2016, revised 22 March 2017, accepted 4 May 2017)

doi:10.1111/febs.14100

Podocytes play an important role in maintaining glomerular function, and podocyte injury is a significant component in the pathogenesis of proteinuria. Soluble epoxide hydrolase (sEH) is a cytosolic enzyme whose genetic deficiency and pharmacological inhibition have beneficial effects on renal function, but its role in podocytes remains unexplored. The objective of this study was to investigate the contribution of sEH in podocytes to lipopolysaccharide (LPS)-induced kidney injury. We report increased sEH transcript and protein expression in murine podocytes upon LPS challenge. To determine the function of sEH in podocytes *in vivo* we generated podocyte-specific sEH-deficient (pod-sEHKO) mice. Following LPS challenge, podocyte sEH-deficient mice exhibited lower kidney injury, proteinuria, and blood urea nitrogen concentrations than controls suggestive of preserved renal function. Also, renal mRNA and serum concentrations of inflammatory cytokines IL-6, IL-1β, and TNFα were significantly lower in LPS-treated pod-sEHKO than control mice. Moreover, podocyte sEH deficiency was associated with decreased LPS-induced NF-κB and MAPK activation and attenuated endoplasmic reticulum stress. Furthermore, the protective effects of podocyte sEH deficiency *in vivo* were recapitulated in E11 murine podocytes treated with a selective sEH pharmacological inhibitor. Altogether, these findings identify sEH in podocytes as a contributor to signaling events in acute renal injury and suggest that sEH inhibition may be of therapeutic value in proteinuria.

Enzymes
Soluble epoxide hydrolase: EC 3.3.2.10.

Abbreviations
ACR, albumin to creatinine ratio; BUN, blood urea nitrogen; CMJ, corticomedullary junction; DHETs, dihydroxyepoxyeicosatrienoic acids; EETs, epoxyeicosatrienoic acids; GBM, glomerular basement membrane; LPS, lipopolysaccharides; sEHIs, sEH pharmacological inhibitors; sEH, soluble epoxide hydrolase.

Introduction

Glomerular disease is characterized by abnormalities in the glomerular matrix and podocytes [1]. Podocytes are the major gatekeeper of glomerular filtration and play a crucial role in maintaining the integrity of the glomerular basement membrane (GBM). These differentiated epithelial cells possess a unique and complex organization that renders them vulnerable to stress. Alterations in podocyte cytoskeleton and migration over the GBM result in effacement of foot processes and apical displacement of the slit diaphragm leading to proteinuria [2]. Proteinuria is an early marker of podocyte injury and an indicator of renal disease. Additionally, proteinuria is often detected before the decline in glomerular filtration rate. Undetected or left untreated, proteinuria may progress to chronic kidney disease and even renal failure [3].

Soluble epoxide hydrolase (sEH, encoded by *Ephx2*) is a conserved cytosolic enzyme that is highly expressed in the kidney, liver, and vasculature [4]. The best understood physiological role of sEH is its metabolism of polyunsaturated fatty acid epoxides into their corresponding diols; including the conversion of anti-inflammatory epoxyeicosatrienoic acids (EETs) into dihydroxyepoxyeicosatrienoic acids (DHETs) [5]. For most biological endpoints, EETs are biologically more active than DHETs, which are rapidly conjugated and excreted [5]. Accordingly, sEH is a major determinant of EETs bioavailability and a regulator of numerous biological processes. Studies using whole-body sEH-deficient mice and selective sEH pharmacological inhibitors (sEHIs) provide insights into the functions of sEH. Pharmacological inhibition of sEH stabilizes EETs and other epoxy fatty acid levels by preventing their conversion into DHETs or corresponding diols [6]. Inhibition of sEH *in vivo* is associated with a variety of beneficial biological outcomes in distinct rodent disease models including renal disease. Indeed, inhibition of sEH reduces inflammation and renal injury in salt-sensitive hypertension and hypertensive type 2 diabetic rats [7–9]. Also, sEH inhibition attenuates renal interstitial fibrosis in the unilateral ureteral obstruction mouse model [10]. Whole-body sEH-deficient mice exhibit reduced renal inflammation in DOCA-salt hypertension model [11] and reduced renal injury in the streptozotocin-induced diabetic mouse model [12]. These studies implicate sEH in renal function, but the role of sEH in podocytes and its contribution to proteinuria and renal injury, if any, remain unclear. In the current study, we investigated the role of sEH in podocytes in lipopolysaccharides (LPS)-induced renal injury using genetic and pharmacological approaches and deciphered the underlying molecular mechanisms.

Results

LPS challenge increases renal and podocyte sEH expression

We determined sEH expression in kidneys and podocytes of wild-type mice under basal (saline) and LPS-treated states. LPS treatment increased renal sEH expression at both transcript and protein levels concomitant with decreased nephrin (a key podocyte protein) expression as previously reported (Fig. 1A) [13]. Also, sEH transcript and protein expression increased in podocytes of wild-type mice after LPS challenge (Fig. 1B). Moreover, sEH expression was determined in E11 murine kidney podocytes treated with LPS for 6, 12, 18, and 24 h. Immunoblotting revealed a significant time-dependent, LPS-induced increase in sEH expression concomitant with a decrease in nephrin expression (Fig. 1C). In total, these findings establish regulation of renal sEH expression upon LPS challenge and suggest that dysregulation of sEH signaling may be relevant to podocyte injury.

Podocyte-specific sEH deficiency preserves renal function under LPS challenge

Lipopolysaccharide-induced upregulation of sEH suggests that it may contribute to signaling events in podocyte injury. To investigate the potential role of sEH in proteinuria, we generated mice with podocyte-specific sEH disruption by crossing $sEH^{fl/fl}$ mice to podocin-Cre transgenic mice as detailed in methods (Fig. 2A–C) [14]. Podocyte sEH-deficient mice (hereafter termed pod-sEHKO) survived to adulthood and did not display gross defects in the kidneys. Immunoblots of isolated podocytes from control and pod-sEHKO mice revealed a significant reduction of sEH expression in deficient mice compared with controls (Fig. 2D). sEH expression in other tissues (adipose, liver, and muscle) was comparable between genotypes suggesting specificity of deletion. Similarly, *Ephx2* expression was significantly reduced in podocytes of sEH-deficient mice compared with controls (Fig. 2E). Also, coimmunostaining of sEH in kidney sections of control and pod-sEHKO mice demonstrated a significant reduction of sEH in podocytes of sEH-deficient mice (Fig. 2F). Thus, pod-sEHKO mice exhibit efficient and specific sEH genetic disruption in podocytes and present a suitable experimental model for investigating the potential contribution of sEH in podocytes to acute renal injury.

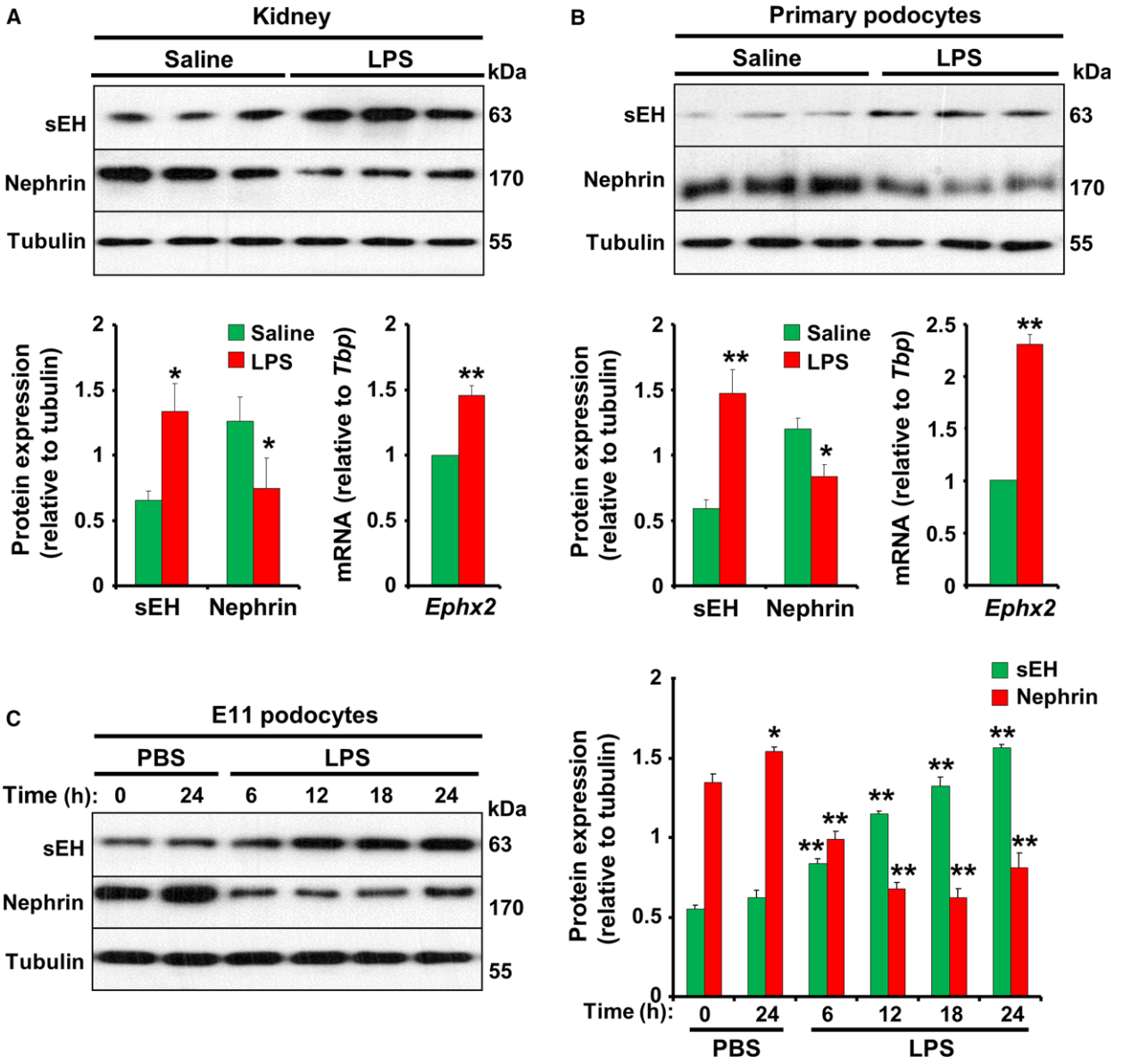

Fig. 1. LPS treatment increases sEH expression in podocytes. (A) Immunoblots of sEH, nephrin, and tubulin in total kidney lysates of control (saline-treated) and LPS-treated C57BL/6J wild-type male mice. Representative immunoblots are shown, and each lane represents an animal. Bar graphs represent protein (left panel) and mRNA (right panel) in kidney lysates from control (saline; $n = 6$) and LPS-treated (LPS; $n = 9$) mice and presented as means + SEM. (B) Lysates of podocytes isolated from control and LPS-treated C57BL/6J wild-type male mice were immunoblotted for sEH, nephrin, and tubulin. Representative immunoblots are shown. Bar graphs represent protein expression (left panel) and mRNA (right panel) in podocytes and presented as means + SEM. In (A) and (B) $*P < 0.05$, $**P < 0.01$ indicate a significant difference between saline- and LPS-treated mice. (C) sEH, nephrin and tubulin protein expression in differentiated murine E11 podocytes without (PBS) and with LPS treatment for the indicated times. Bar graph represents sEH and nephrin expression and presented as means + SEM from three independent experiments. $*P < 0.05$, $**P < 0.01$ indicate a significant difference between PBS (24 h) and LPS-treated groups at the shown time versus PBS (0 h).

Lipopolysaccharide treatment of control and pod-sEHKO mice decreased body weight of both genotypes but to a lesser extent in the latter (Fig. 3A). Moreover, LPS increased kidney weights in both genotypes but to a lower level in pod-sEHKO mice (Fig. 3B,C). Urinary proteins were very low in both control and pod-sEHKO mice prior to LPS challenge (Fig. 3D). LPS treatment significantly increased urinary proteins and urinary albumin/creatinine, but they were lower in pod-sEHKO mice suggestive of preserved filter integrity and renal

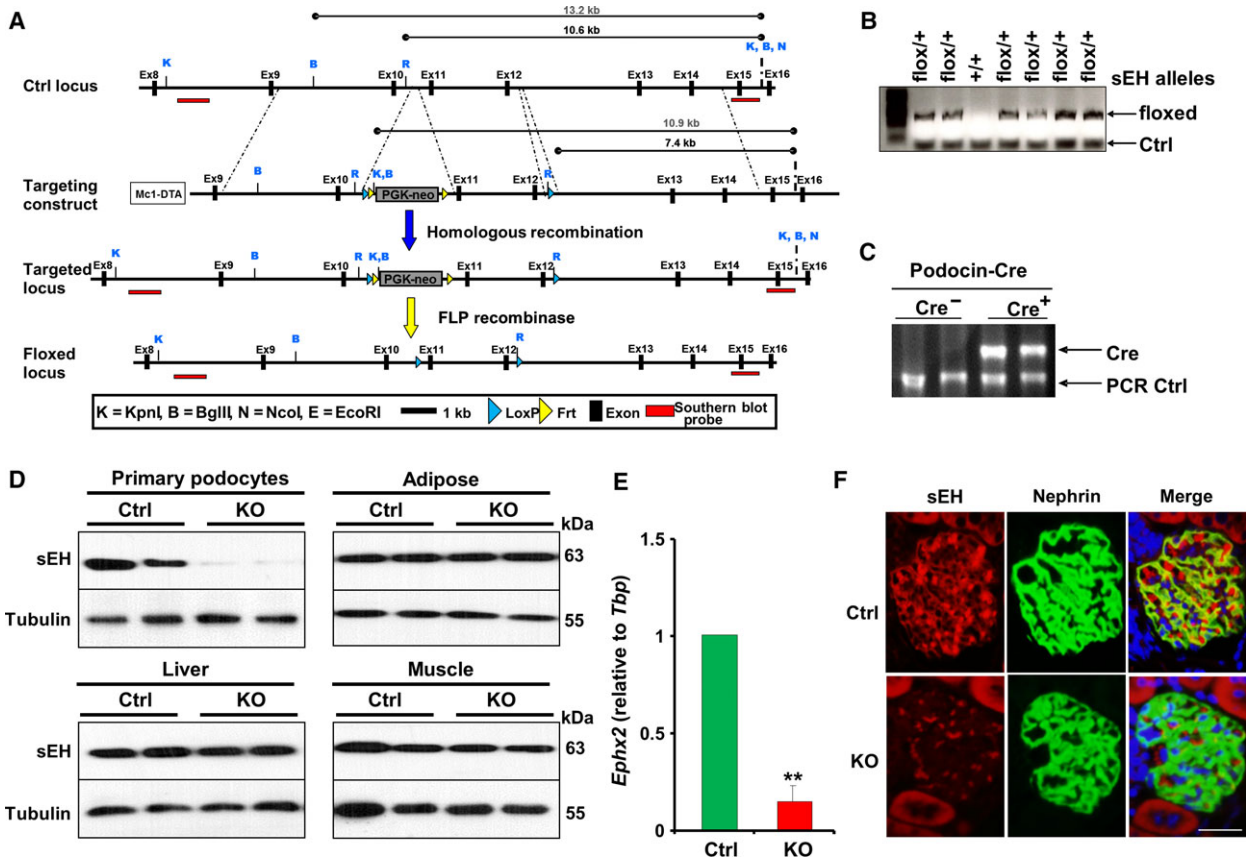

Fig. 2. Efficient and specific deletion of sEH in podocytes. (A) sEH genomic locus and targeting; two loxP sites were designed in an intronic region of the sEH gene. (B–C) Confirmation of sEH floxed and Cre mice by PCR. Genomic DNA from tails was amplified by PCR; primers were designed to distinguish the alleles with and without loxP insertions (B), and Cre (C). (D) Immunoblots of sEH expression in podocytes, epididymal fat, liver, and muscle of control (Ctrl) and pod-sEHKO (KO) mice. Representative immunoblots are shown. (E) *Ephx2* expression in podocytes of control (Ctrl; $n = 6$) and pod-sEHKO (KO; $n = 6$) mice. $^{**}P < 0.01$ indicates a significant difference between Ctrl and KO. (F) Co-immunostaining of sEH (red) and nephrin (green) in kidney paraffin sections of Ctrl and KO mice. Scale bar: 200 μm.

function (Fig. 3D,E). Similarly, and in line with previous reports [15,16] LPS caused a marked elevation in blood urea nitrogen (BUN) levels, but that was lower in pod-sEHKO mice consistent with preserved renal function (Fig. 3F). Furthermore, and consistent with published reports [17–19] LPS led to a significant decrease in serum albumin levels with concomitant elevated serum creatinine in control mice (Fig. 3G,H). Podocyte sEH deficiency mitigated changes in serum albumin and creatinine levels. Of note, the renal protective effects of podocyte sEH deficiency were also observed in a second model (anti-GBM serum treatment of female mice) as evidenced by urinary albumin/creatinine and BUN levels (Fig. 3I,J). As early stages of proteinuric diseases show evidence of glomerular injury and tubular impairment [20], we evaluated histological changes in PAS-stained kidney sections from control and pod-sEHKO mice under basal (saline) and LPS-treated states. The most noticeable morphological changes included acute tubular injury and Bowman space dilatation which were diffusely involving renal parenchyma in LPS-treated control mice, and very focal in control and pod-sEHKO mice with LPS administration (Fig. 3K, Table 1). Importantly, LPS-treated pod-sEHKO mice exhibited significantly less tubular injury and Bowman space dilatation. Finally, immunostaining of nephrin in kidney sections of control mice revealed decreased nephrin expression upon LPS challenge (Fig. 3L), consistent with biochemical findings (in Fig. 1) and published studies [21]. However, podocyte sEH deficiency mitigated the effects of LPS and prevented the decrease in nephrin expression. Altogether, the aforementioned findings establish a protective effect of podocyte sEH deficiency in LPS-induced proteinuria and identify podocytes as significant contributors to the beneficial effects of sEH deficiency.

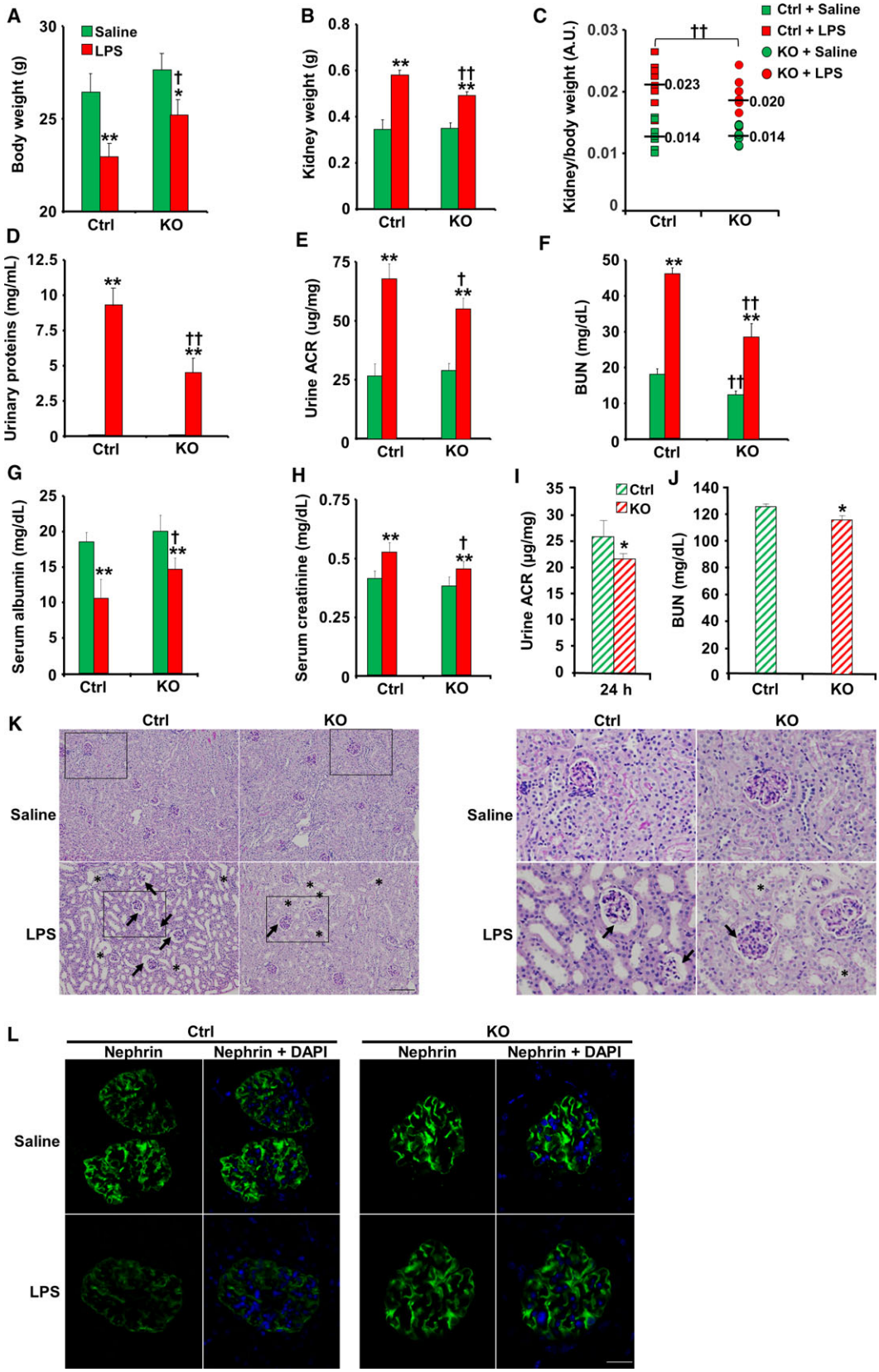
A
Body weight (g)
Saline
LPS
Ctrl
KO
B
Kidney weight (g)
C
Kidney/body weight (A.U.)
Ctrl + Saline
Ctrl + LPS
KO + Saline
KO + LPS
0.023
0.020
0.014
0.014
D
Urinary proteins (mg/mL)
E
Urine ACR (ug/mg)
F
BUN (mg/dL)
G
Serum albumin (mg/dL)
H
Serum creatinine (mg/dL)
I
Urine ACR (μg/mg)
24 h
J
BUN (mg/dL)
K
Saline
LPS
L
Nephrin
Nephrin + DAPI

Fig. 3. Podocyte sEH deficiency attenuates LPS-induced proteinuria. Body (A) and kidney (B) weights, and kidney to body weight ratio (C) of control (Ctrl) and pod-sEHKO (KO) mice without (saline) and with LPS treatment. Urinary proteins (D), ACR (E), BUN (F), serum albumin (G), and creatinine (H) from control and pod-sEHKO mice without (saline) and with LPS treatment ($n = 9$ per group). $^{*}P < 0.05$, $^{**}P < 0.01$ indicate a significant difference between mice without and with LPS treatment, and $^{\dagger}P < 0.05$, $^{\dagger\dagger}P < 0.01$ indicate a significant difference between pod-sEHKO and control mice. ACR (I) and BUN (J) from control and pod-sEHKO female mice ($n = 5$–6/group) after anti-GBM serum injection. $^{*}P < 0.05$ indicates a significant difference between pod-sEHKO and control mice. (K) PAS-stained kidney sections of Ctrl and pod-sEHKO mice without and with LPS treatment. Arrows indicate dilated Bowman space and asterisks indicate dilated tubules. Scale bar: 200 μm. Images in the right panel are a magnification of the boxed regions. (L) Immunostaining for nephrin (green), and DAPI (blue) in kidney sections of control Ctrl and pod-sEHKO mice without and with LPS treatment. Scale bar: 50 μm.

Table 1. Histological evaluation of injury in PAS-stained kidney sections of control and pod-sEHKO mice. Tubules from the cortex and CMJ regions were examined in PAS-stained kidney sections of control (Ctrl) and pod-sEHKO (KO) mice without (saline), and with LPS treatment and were scored as described in methods. The extent of injury was calculated as follows (number of tubules with a score higher than 0 × corresponding score)/total number of tubules examined (e.g.,: the extent of tubules injury in WT-LPS = [(217 × 2) + (637 × 1)]/854 = 1.254).

	WT-saline ($n = 4$)	WT-LPS ($n = 4$)	KO-saline ($n = 4$)	KO-LPS ($n = 8$)
Cortex				
Number of tubules examined	764	854	883	1399
Injury score				
7	637	10	80	80
0	217	0	0	0
0	0	0	0	0
0	0	0	1	2
Extent of injury	0.009	1.254	0.011	0.060
CMJ				
Number of tubules examined	781	824	841	1391
Injury score				
16	588	59	88	88
0	118	4	6	12
0	3	0	0	0
0	0	3	1	4
Extent of injury	0.020	1.102	0.093	0.066

Podocyte sEH deficiency mitigates LPS-induced inflammation

Lipopolysaccharide treatment increases renal and systemic cytokine concentrations [22] and systemic inflammatory response [23]. Accordingly, we investigated the effects of podocyte-specific sEH disruption on LPS-induced alterations in inflammatory cytokines, namely interleukin-1β (IL-1β), interleukin-6 (IL-6), and tumor necrosis factor-α (TNFα). Renal mRNA and serum concentrations of IL-1β, IL-6, and TNFα were elevated in both control and pod-sEHKO mice after LPS challenge but were significantly lower in the latter (Fig. 4A,B). The nuclear factor-kappa B (NF-κB) plays a significant role in the regulation of IL-1β and TNFα during LPS-induced renal injury [24,25]. Also, sEH deficiency leads to anti-inflammatory effects through attenuation of NF-κB signaling [26]. Accordingly, we examined renal NF-κB signaling in control and pod-sEHKO mice under basal and LPS-treated states. LPS-induced IKKα, IκBα, and NF-κBp65 phosphorylation and NF-κBp50 expression were significantly less in pod-sEHKO mice compared with controls (Fig. 4C). This finding is in line with the reduced proinflammatory cytokines in pod-sEHKO mice.

Activation of mitogen-activated protein kinases (MAPKs) including JNK and p38 has been reported in human renal diseases [27,28]. Also, pharmacological inhibition of JNK or p38 suppresses proteinuria and renal injury through attenuating renal inflammation and fibrosis [27,29,30]. Accordingly, we examined the activation of JNK and p38 in control and pod-sEHKO mice under basal and LPS-treated states. LPS treatment increased JNK and p38 phosphorylation in both control and pod-sEHKO mice but that was significantly lower in the latter (Fig. 4D). Collectively, these findings establish decreased LPS-induced inflammatory response in pod-sEHKO mice and are consistent with the protective effects of podocyte sEH deficiency in LPS-induced renal injury.

Podocyte sEH deficiency attenuates LPS-induced endoplasmic reticulum stress

Endoplasmic reticulum (ER) stress plays a significant role in the progression of proteinuria [31] and apoptosis in response to severe proteinuria [32]. sEH deficiency and pharmacological inhibition attenuate ER stress in liver, adipose tissue [26,33], and pancreas [34,35]. Thus, we examined alterations in ER stress in control and pod-sEHKO mice under basal and LPS-treated states. Consistent with published reports [36–38], LPS induced renal ER stress as evidenced by

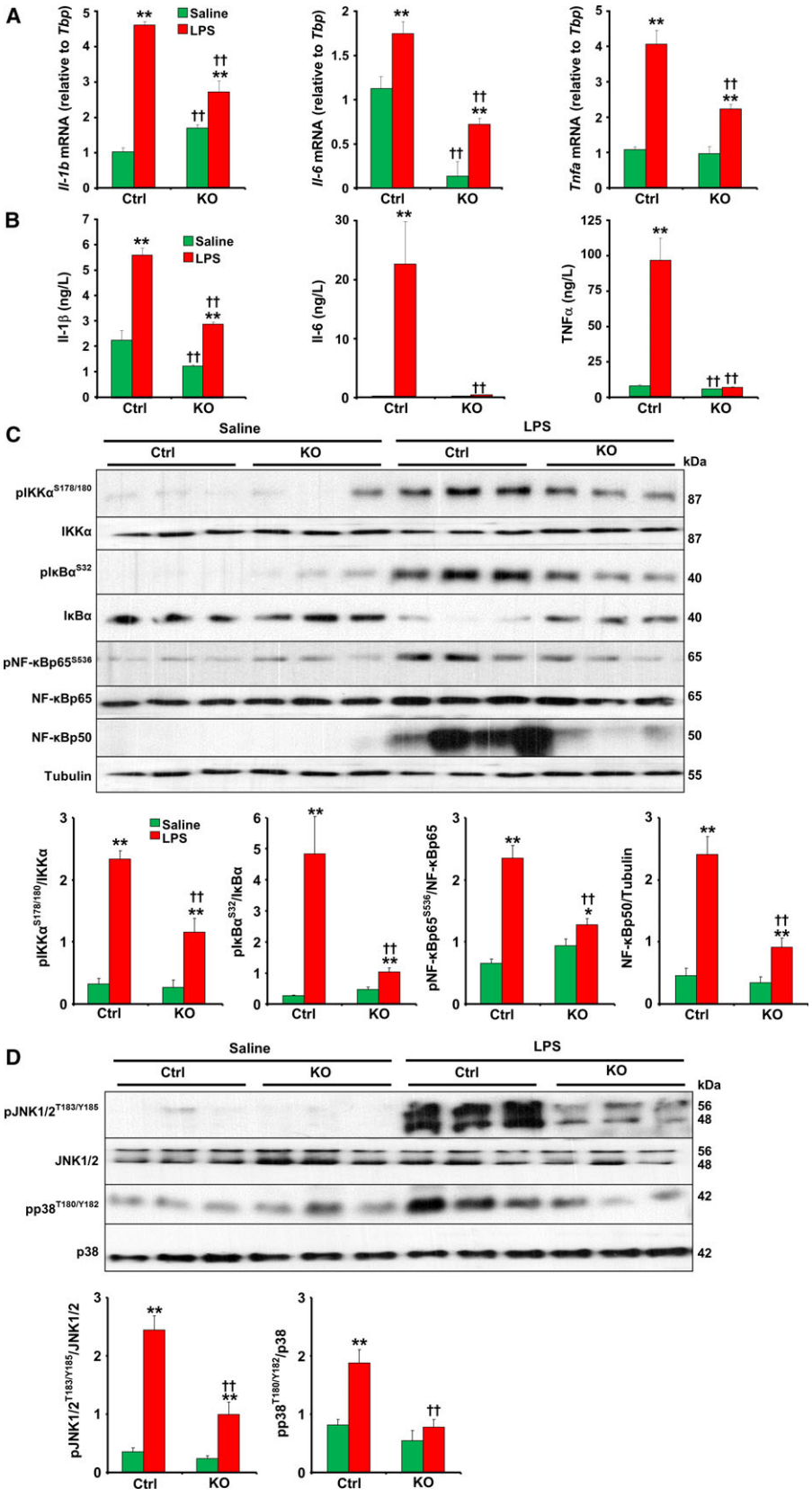
A
Saline
LPS
Il-1b mRNA (relative to Tbp)
Il-6 mRNA (relative to Tbp)
Tnfa mRNA (relative to Tbp)
Ctrl
KO
B
Il-1β (ng/L)
Il-6 (ng/L)
TNFα (ng/L)
C
Saline
LPS
Ctrl
KO
kDa
pIKKα S178/180
IKKα
pIκBα S32
IκBα
pNF-κBp65 S536
NF-κBp65
NF-κBp50
Tubulin
87
87
40
40
65
65
50
55
pIKKα S178/180/IKKα
pIκBα S32/IκBα
pNF-κBp65 S536/NF-κBp65
NF-κBp50/Tubulin
D
pJNK1/2 T183/Y185
JNK1/2
pp38 T180/Y182
p38
56
48
56
48
42
42
pJNK1/2 T183/Y185/JNK1/2
pp38 T180/Y182/p38

Fig. 4. Decreased LPS-induced inflammatory response in podocyte sEH-deficient mice. Renal mRNA (A) and serum (B) levels of IL-1β, IL-6, and TNFα in saline- and LPS-treated control ($n = 6$) and pod-sEHKO ($n = 6$) mice. Serum IL-6 concentration was very low in both control and pod-sEHKO mice before LPS challenge. (C) Kidney lysates from control and pod-sEHKO mice without (saline) and with LPS treatment were immunoblotted for pIKKα, pIκBα, pNF-κBp65, their respective unphosphorylated proteins, and Tubulin as a loading control. Representative immunoblots are shown. Bar graphs represent pIKKα/IKKα, pIκBα/IκBα, pNF-κBp65/NF-κBp65, and NF-κBp50/Tubulin as means + SEM. (D) Kidney lysates from control and pod-sEHKO were immunoblotted for pJNK and pp38 and their respective unphosphorylated proteins. Representative immunoblots are shown. Bar graphs represent pJNK/JNK and pp38/p38 as means + SEM. $^{*}P < 0.05$, $^{**}P < 0.01$ indicate a significant difference between mice without (saline) and with LPS treatment, and $^{\dagger}P < 0.05$, $^{\dagger\dagger}P < 0.01$ indicate a significant difference between pod-sEHKO and control mice.

elevated activation of ER transmembrane proteins PKR-like ER-regulated kinase (PERK) and inositol-requiring enzyme 1α (IRE1α), and their respective downstream targets α-subunit of eukaryotic translation initiation factor 2 (eIF2α) and X-box binding protein 1 (XBP1) (Fig. 5). Importantly, pod-sEHKO mice exhibited attenuated LPS-induced ER stress as evidenced by decreased PERK (Thr980), eIF2α (Ser51), and IRE1α (Ser724) phosphorylation and XBP1 splicing. Also, pod-sEHKO mice exhibited decreased LPS-induced caspase3 cleavage compared with controls. These data establish attenuated LPS-induced renal ER stress in podocyte sEH-deficient mice.

sEH pharmacological inhibition *in vitro* recapitulates the protective effects of podocyte sEH disruption

The renal response to LPS-induced injury encompasses many cell types that include glomerular podocytes [39]. To delineate the contribution of sEH in podocytes to LPS-induced injury we used immortalized E11 murine podocytes [40]. Differentiated E11 podocytes were treated with the selective sEH inhibitor TPPU as detailed in methods, and the effects on LPS-induced inflammatory response and ER stress were evaluated. LPS induced activation of NF-κB and MAPK signaling as well as the elevation of ER stress in E11 podocytes (Fig. 6A,B). Importantly, sEH pharmacological inhibition mitigated the deleterious effects of LPS treatment in these cells. Indeed, sEH inhibitor-treated E11 podocytes exhibited lower LPS-induced activation of NF-κB and MAPK as evidenced by decreased IKKα, IκBα, NF-κBp65, JNK, and p38 phosphorylation (Fig. 6A). Similarly, sEH inhibitor-treated podocytes exhibited lower LPS-induced ER stress as evidenced by decreased PERK, eIF2α, and IRE1α phosphorylation, and decreased sXBP1 splicing and caspase3 cleavage (Fig. 6B). These findings are in keeping with observations in pod-sEHKO mice and are consistent with autonomous cell effects.

Discussion

Podocytes function under numerous physiological and pathophysiological stresses to maintain the integrity of the glomerular filtration barrier. Podocytes adapt to maintain homeostasis, but excessive stress can cause podocyte dysfunction and injury that lead to proteinuria and glomerulosclerosis. The complex cellular and molecular mechanisms underlying podocyte injury and its consequences are not well understood. In the current study, we investigated the potential contribution of sEH in podocytes to acute renal injury using genetic and pharmacological approaches. LPS induced upregulation in sEH transcript and protein levels in podocytes. Remarkably, podocyte-specific sEH disruption significantly attenuated LPS-induced renal dysfunction and was associated with decreased NF-κB inflammatory response, MAPK and ER stress signaling. In addition, the *in vivo* protective effects of podocyte sEH deficiency were recapitulated *in vitro* in immortalized podocytes treated with a selective sEHI. Collectively, these findings identify sEH as a significant contributor to signaling events following podocyte injury and suggest that sEH inhibition in podocytes may be of therapeutic value in proteinuria.

Several studies implicate the Arachidonic acid cytochrome P450 epoxygenase pathway in glomerular function and establish a correlation between the decline in glomerular function and concentrations of EETs. Streptozotocin-induced diabetes in rats causes a significant decrease in glomerular 20-HETE and EETs concomitant with increased proteinuria and glomerular hypertrophy [41]. Also, upregulation of sEH in proximal tubular cells mediates proteinuria-induced renal damage [42], while sEH inhibition markedly ameliorates proteinuria-induced epithelial–mesenchymal transition [43]. Moreover, genetic disruption of *Ephx2* decreases inflammation and attenuates albuminuria and renal damage associated with salt-sensitive hypertension [44]. Furthermore, sEH deficiency and pharmacological inhibition prevent renal interstitial fibrosis in unilateral ureteral obstruction models [10,45]. In

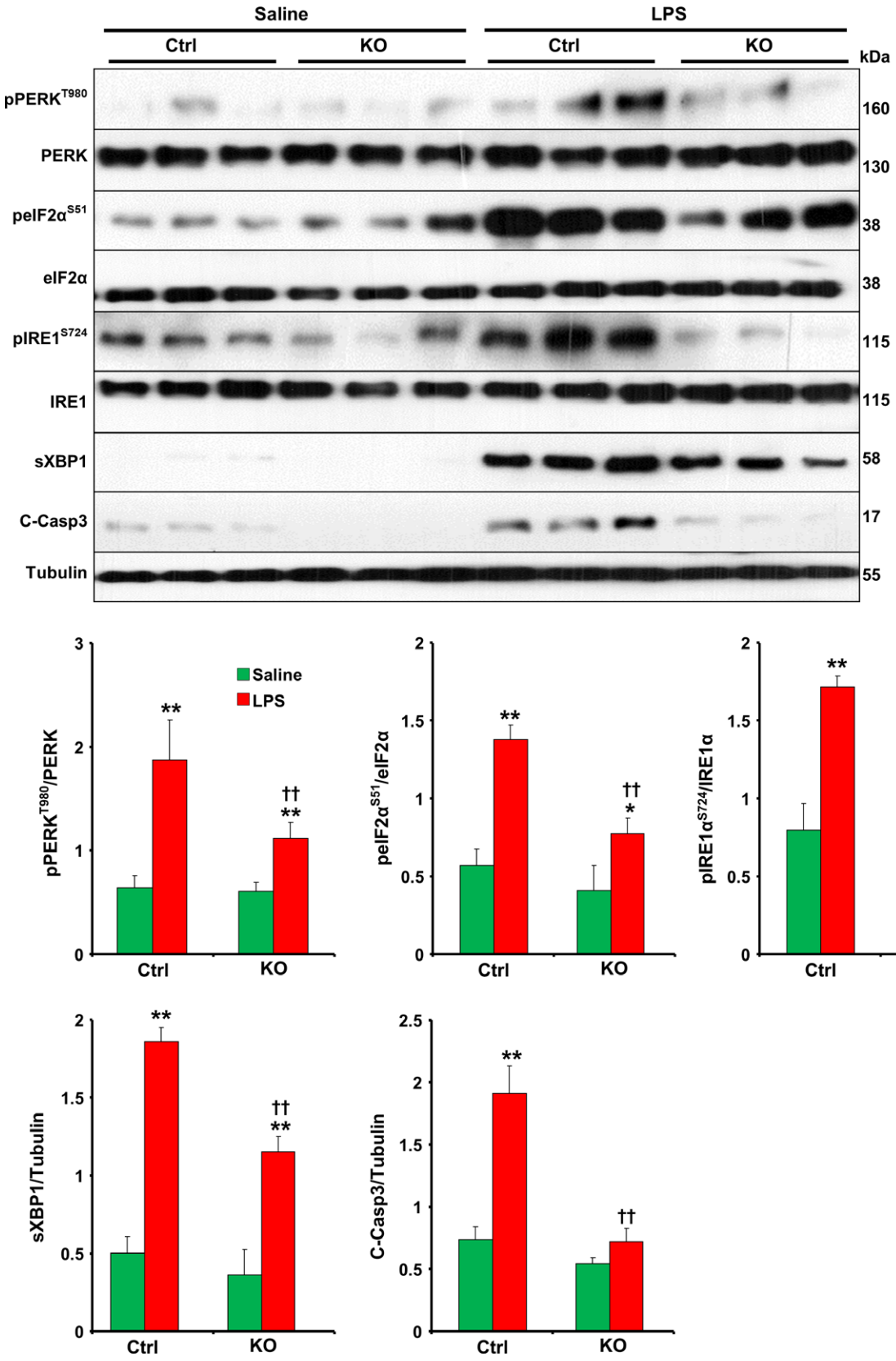
Saline
LPS
Ctrl
KO
Ctrl
KO
kDa
pPERK^{T980}
PERK
peIF2α^{S51}
eIF2α
pIRE1^{S724}
IRE1
sXBP1
C-Casp3
Tubulin
160
130
38
38
115
115
58
17
55
Saline
LPS
pPERK^{T980}/PERK
peIF2α^{S51}/eIF2α
pIRE1α^{S724}/IRE1α
sXBP1/Tubulin
C-Casp3/Tubulin
Ctrl
KO

Fig. 5. Decreased LPS-induced ER stress in podocyte sEH-deficient mice. Immunoblots of key proteins in ER stress signaling in kidney lysates from saline- and LPS-treated control and pod-sEHKO mice ($n = 6$/group). Representative immunoblots are shown. Bar graphs of pPERK/PERK, peIF2α/eIF2α, pIRE1α/IRE1α, sXBP1/Tubulin, and cleaved caspase3/Tubulin are presented as means + SEM. $^{*}P < 0.05$, $^{**}P < 0.01$ indicate a significant difference between mice without (saline) and with LPS treatment, and $^{\dagger\dagger}P < 0.01$ indicates a significant difference between pod-sEHKO and control mice.

keeping with these reports, the current findings establish a protective role for podocyte-specific sEH disruption in acute renal injury. Importantly, the protective effects of sEH deficiency were observed in two different mouse models of renal injury including males and females, demonstrating that they were not specific to particular challenge or gender. Furthermore, the effects of podocyte sEH deficiency were recapitulated in podocytes treated with a selective sEH inhibitor consistent with autonomous effects, but we cannot rule out the potential contribution of other cell types to the LPS response. It is worth nothing that the current studies harbor some limitations. The reagent used in Bradford assay does not react with urinary proteins that are smaller than 13 kDa [46]. However, since most proteins that appear in the urine of patients with glomerular proteinuria are of intermediate size [39,47–52], the used methodology is likely suitable. Indeed, the current findings on the effect of LPS on albumin and albumin to creatinine ratio (ACR) in control mice are consistent with published reports [21,53,54]. Also, we cannot rule out that the urinary proteins could have nonfiltration related causes. Moreover, changes in serum albumin upon LPS challenge are unlikely to be due to filtration alone as previous studies demonstrate inhibition of albumin tubular transcytosis [55], an essential mechanism to preserve serum albumin levels, in response to acute kidney injury [56,57]. Nevertheless, the current findings and previous reports suggest that inhibiting sEH to increase EETs and other epoxy fatty acids may be of value in combating glomerular injury.

Previous studies implicate podocytes in LPS-induced proteinuria [39]. Herein, we demonstrate that podocyte-specific sEH genetic disruption *in vivo* and pharmacological inhibition in podocytes were associated with decreased LPS-induced inflammation, MAPK activation, and ER stress. Inflammation in the glomeruli leads to proteinuria [58], and activation of NF-κB during proteinuric diseases and renal injury has been documented in glomeruli [59–61]. Therefore, it is reasonable to stipulate that the protective effects of podocyte-specific sEH disruption against acute renal injury and proteinuria may be mediated, at least partly, by decreased activation of NF-κB signaling. The underlying mechanism through which sEH deficiency attenuates NF-κB signaling remains to be delineated but can be related to an overall reduction in inflammation. The current findings are in line with reports of reduced renal inflammation in streptozotocin-treated sEH whole-body knockout mice and sEHI-treated diabetic mice [12]. Also, podocyte-specific sEH disruption and pharmacological inhibition impacted other pathways that contribute to proteinuric kidney disease, namely ER stress. ER stress is evoked in several kidney diseases (such as membranous nephropathy, proteinuric renal diseases, and renal fibrosis) and attenuation of ER stress decreases proteinuria and interstitial fibrosis and restores renal integrity [62–67]. Similarly, administration of the chaperone 4-phenylbutyrate to mitigate ER stress is associated with improvement in tubular lesions [62]. Thus, attenuated ER stress *in vivo* upon podocyte sEH deficiency and inhibition is in line with the renal protective effects of podocyte sEH deficiency. These findings are consistent with our previous studies demonstrating that sEH deficiency and inhibition attenuate HFD-induced ER stress in liver and adipose tissue [33], and in the pancreas during acute pancreatitis [34,35]. The mechanism underlying attenuation of ER stress by sEH deficiency is unclear but may encompass an increase in EETs and other epoxy fatty acids and/or decrease in diols, although this still needs to be demonstrated. As such, upregulation of sEH in podocytes after LPS challenge may decrease the concentration of EETs and increase the diols thereby contributing to elevated ER stress during podocyte injury. Additional investigation is needed to decipher the contribution of sEH to ER stress-mediated podocyte injury and consequences on proteinuric kidney diseases. Nevertheless, the current study establishes protective effects of podocyte-specific sEH deficiency against LPS-induced renal injury and suggests that sEH inhibition in podocytes may have potential therapeutic implications for combating podocyte injury.

Materials and methods

Reagents

RPMI medium, penicillin/streptomycin, and trypsin were purchased from Invitrogen (Carlsbad, CA, USA). FBS was purchased from Gemini Bio-Products (Sacramento, CA,

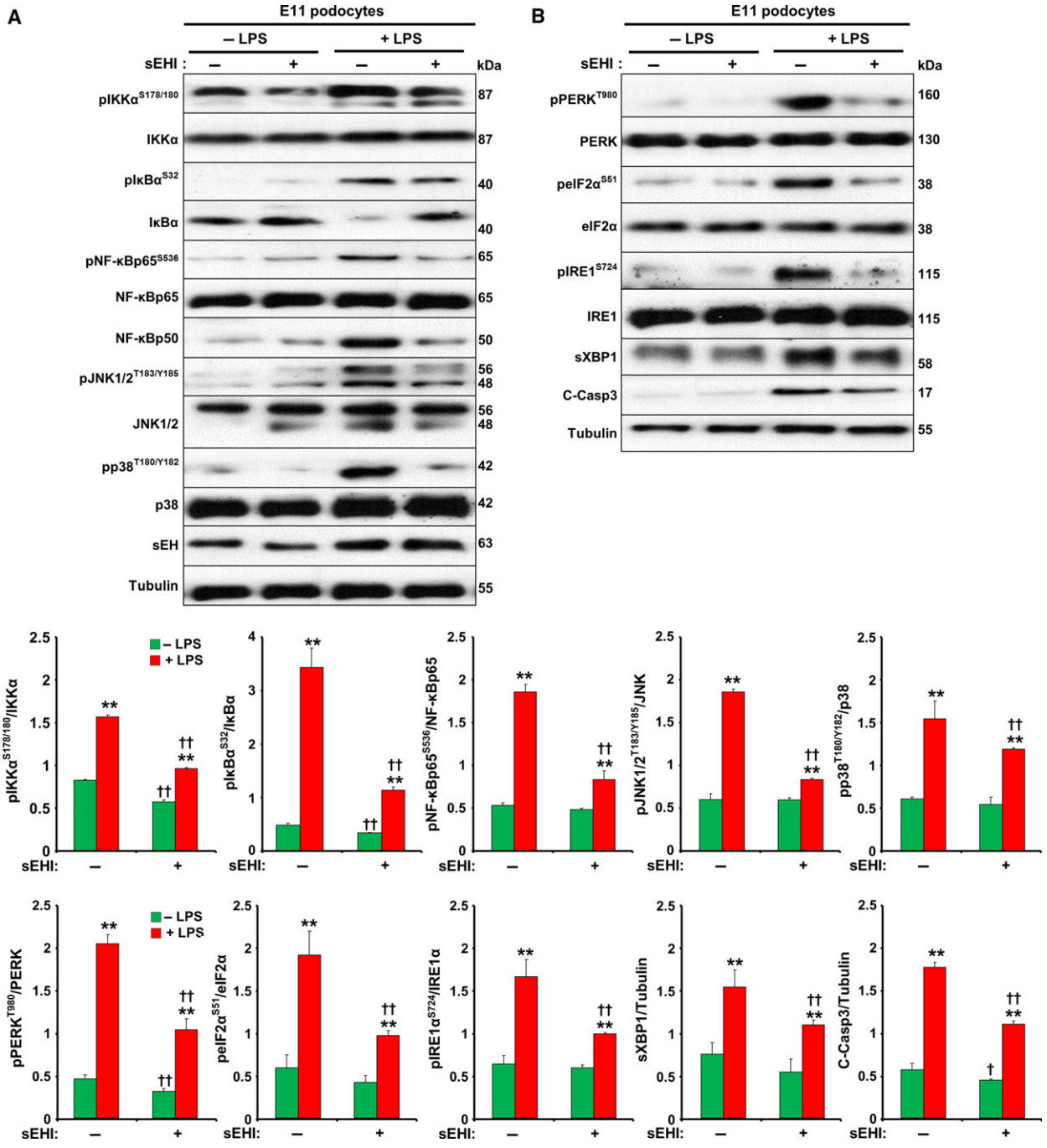

Fig. 6. Pharmacological inhibition of sEH attenuates LPS-induced inflammatory and ER stress signaling in immortalized podocytes. Immunoblots of key proteins in inflammation, MAPK, and ER stress signaling in differentiated E11 podocytes without (−LPS) and with (+LPS) treatment for 24 h and without (–) and with (+) sEH pharmacological inhibition (sEHI). Representative immunoblots are shown. Bar graphs of pIKKα/IKKα, pIκBα/IκBα, pNF-κBp65/NF-κB, NF-κBp50/Tubulin, pJNK/JNK, pp38/p38, pPERK/PERK, peIF2α/eIF2α, pIRE1α/IRE1α, sXBP1/Tubulin, and cleaved Caspase3/Tubulin are presented as means + SEM from three independent experiments. $^{**}P < 0.01$ indicates a significant difference in cells without and with LPS treatment. $^{\dagger}P < 0.05$, $^{\dagger\dagger}P < 0.01$ indicate a significant difference between nontreated and sEHI-treated cells.

USA). Antibodies used in this study (sources, species, and conditions of use) are listed in Table 2. Nephrotoxic antisera (sheep anti-rat GBM) were purchased from Probetex (San Antonio, TX, USA). Unless otherwise indicated, chemicals were purchased from Sigma-Aldrich (St. Louis, MO, USA).

Table 2. List of primary and secondary antibodies and conditions of use.

Antibodies	Source	Host	Dilution
β-Tubulin	Santa Cruz Biotechnology (Santa Cruz, CA, USA)	Mouse	1 : 20 000
Cleaved Caspase 3	Cell Signaling Technology (Danvers, MA, USA)	Rabbit	1 : 5000
eIF2α	Santa Cruz Biotechnology	Mouse	1 : 500
IKKα	Cell Signaling Technology	Rabbit	1 : 2500
IRE1	Santa Cruz Biotechnology	Rabbit	1 : 1000
IκBα	Cell Signaling Technology	Rabbit	1 : 2500
JNK1/2	Santa Cruz Biotechnology	Rabbit	1 : 5000
Nephrin (used for IF)	Santa Cruz Biotechnology	Goat	1 : 100
Nephrin (used for WB)	Santa Cruz Biotechnology	Rabbit	1 : 1000
NF-κB p65	Cell Signaling Technology	Rabbit	1 : 5000
NF-κB p50	Cell Signaling Technology	Rabbit	1 : 2500
p38	Santa Cruz Biotechnology	Rabbit	1 : 5000
peIF2α^{S51}	Santa Cruz Biotechnology	Rabbit	1 : 1000
PERK	Santa Cruz Biotechnology	Rabbit	1 : 1000
pIKKα$^{S178/180}$	Cell Signaling Technology	Rabbit	1 : 2500
pIRE1^{S724}	Abcam (Cambridge, MA, USA)	Rabbit	1 : 10 000
pIκBα^{S32}	Cell Signaling Technology	Rabbit	1 : 2500
pJNK1/2$^{T183/Y185}$	Cell Signaling Technology	Rabbit	1 : 10 000
pNF-κB p65^{S536}	Cell Signaling Technology	Rabbit	1 : 2500
pp38$^{T180/Y182}$	Cell Signaling Technology	Rabbit	1 : 10 000
pPERK^{T980}	Santa Cruz Biotechnology	Rabbit	1 : 1000
sEH	Dr B. Hammock Laboratory (Davis, CA, USA)	Rabbit	1 : 10 000
sXBP1	Santa Cruz Biotechnology	Goat	1 : 1000

Mouse studies

sEH floxed (*Ephx2*$^{fl/fl}$) mice were generated and kindly provided by D. Zeldin (NIEHS) and were backcrossed on the C57Bl/6J background. Transgenic mice expressing Cre recombinase under control of the podocin promoter on the C57Bl/6J background were purchased from Jackson Laboratories (Sacramento, CA, USA) [14]. sEH floxed mice were bred to podocin-Cre mice to generate podocyte-specific sEH-deficient mice. Genotyping for the *Ephx2* floxed allele and Cre was performed by polymerase chain reaction using DNA from tails. Mice were maintained on a 12-h light-dark cycle with free access to water and standard laboratory chow (Purina Lab, St. Louis, MO, USA chow, #5001). For LPS-induced renal injury, 10–12 week old pod-sEHKO (*Ephx2*$^{fl/fl}$ Pod-cre^{+}) and control (*Ephx2*$^{fl/fl}$) male mice were injected once intraperitoneally with LPS (Sigma-Aldrich; 16 mg·kg^{-1} body weight in 0.9% sterile saline solution). For anti-GBM serum-induced acute kidney injury 8–10-week-old female mice received a single retro-orbital injection of sheep anti-rat GBM serum (5 mL·kg^{-1} body weight diluted in 0.02 M phosphate buffered saline PBS, pH: 7.3) [58]. Mice were sacrificed 24 h after LPS, or 24 and 48 h after anti-GBM serum injections then kidneys were harvested and processed for biochemical and histological analyses. Urine samples were collected 2 h before sacrifice in 50-mL conical tubes. Tubes were centrifuged for 1 min at 1000 ***g*** then urine (80–200 μL) was stored at −80 °C until further analyses. Blood samples (600–800 μL) were collected using the cardiac puncture method at sacrifice. Proteins were measured in 2 μL urine samples using the Bio-Rad Protein Assay reagent (BioRad, Hercules, CA, USA). Also, BUN levels were measured using the Urea Nitrogen Colorimetric Detection Kit from Arbor Assays (Ann Arbor, MI, USA). Serum and urine albumin and creatinine levels were measured using the BCG Albumin and Creatinine Assay Kits (Sigma-Aldrich), respectively, according to manufacturer's instructions. Circulating cytokines were measured using a multiplex electrochemiluminescent assay from Meso Scale Discovery (Rockville, MD, USA). All mouse studies were conducted according to federal regulations and were approved by the Institutional Animal Care and Use Committee at the University of California-Davis.

Histological assessment of renal injury

Kidney sections were fixed in 4% paraformaldehyde, embedded in paraffin, and deparaffinized in xylene, and then 5-μm sections were stained with periodic acid Schiff (PAS) using a commercially available kit (Sigma-Aldrich) according to manufacturer' recommendations. Renal injury was assessed as previously described [68,69] by morphometric analysis of the tubular damage using the following criteria: no injury (score 0), tubular dilatation and brush border loss (score 1), tubular epithelial cells vacuolization (score 2), apical blebbing (score 3), and epithelial cells sloughing (score 4). In each case, 10 high power fields (×40) of renal cortex and corticomedullary junction (CMJ) were scored separately for acute tubular injury. The extent of the damage was calculated as follows (number of tubules with a score higher than 0 × corresponding score)/total number of tubules examined.

Immunofluorescence

Kidneys from control and pod-sEHKO mice were fixed in 10% formalin and embedded in paraffin. Sections were coimmunostained for nephrin, sEH, and DAPI. Detection was performed with appropriate fluorophore-conjugated secondary antibodies (1 : 500; Invitrogen) and visualized using Leica DMI8 inverted microscope (Leica Microsystems Inc., Buffalo Grove, IL, USA).

Podocyte isolation and cell culture

Glomeruli were isolated from control and pod-sEHKO mice using established protocols [70,71] with some

Table 3. List of primers used to quantitate *Ephx2* and proinflammatory cytokines expression.

Gene	Forward 5′->3′	Reverse 5′->3′
Ephx2	CTGGATACCCTGAAGGCAAA	TGACGTCATTTGGATTGCAT
Il-1β	AGCTTCAGGCAGGCAGTATC	AAGGTCCACGGGAAAGACAC
Il-6	ACAACCACGGCCTTCCCTACTT	CACGATTTCCCAGAGAACATGTG
Tbp	TTGGCTAGGTTTCTGCGGTC	GCCCTGAGCATAAGGTGGAA
Tnfα	GACGTGGAACTGGCAGAAGAG	TGCCACAAGCAGGAATGAGA

modifications. Briefly, podocytes were isolated using successive sieving approach. Kidneys were decapsulated and minced in Krebs–Henseleit saline solution (KHS; 119 mM NaCl, 4.7 mM KCl, 1.9 mM $CaCl_2$, 1.2 mM KH_2PO_4, 1.2 mM $MgSO_4{\cdot}7H_2O$, and 25 mM $NaHCO_3$, pH: 7.4). Samples were pelleted at 500 g for 10 min and then washed twice with KHS buffer. Before the second wash, samples were passed through a 250 μm sieve and pelleted at 500 ***g*** for 10 min then digested for 30 min at 37 °C in Hanks buffer containing collagenase D (0.1%), trypsin (0.25%), and DNase I (0.01%). Solutions were filtered through a 100-μm sieve placed above a 53-μm sieve. Podocytes were centrifuged for 5 min at 1500 ***g***, 4 °C and lysed in radioimmunoprecipitation assay (RIPA) buffer. Immortalized E11 murine podocytes (Cell Lines Service, Eppelheim, Germany) were cultured in RPMI containing 11 mM glucose, 10% FBS, 50 $U{\cdot}mL^{-1}$ penicillin, and 50 $\mu g{\cdot}mL^{-1}$ at 33 °C. To induce differentiation, cells were transferred to 37 °C for 14 days [40]. When indicated, podocytes were treated with freshly prepared LPS (10 μM) for 24 h, or sEH inhibitor 1-trifluoromethoxyphenyl-3-(1-propionylpiperidin-4-yl) urea (TPPU; 10 μM) [72,73] 2 h before LPS treatment.

Biochemical analyses

Tissues and cells were lysed in RIPA buffer as described [74]. Lysates were clarified by centrifugation at 13 000 ***g*** for 10 min, and protein concentrations determined using bicinchoninic acid assay kit (Pierce Chemical, Dallas, TX, USA). Proteins (15–30 μg) were resolved by SDS/PAGE and transferred to PVDF membranes. Immunoblotting of lysates was performed with primary antibodies, and after incubation with secondary antibodies, proteins were visualized using Luminata™ Western Chemiluminescent HRP Substrate (Millipore Corp., Billerica, MA, USA). Pixel intensities of immunoreactive bands were quantified using FLUORCHEM Q IMAGING software (Alpha Innotech Corp., San Jose, CA, USA). Data for phosphorylated proteins are presented as phosphorylation normalized to protein expression.

Kidneys from control and pod-sEHKO mice were cut and immediately placed in extraction reagent (TRIzol; Invitrogen). RNA was extracted according to the manufacturer's instructions and resuspended in 50 μL of RNase-free water. The concentration of RNAs was determined using the NanoDrop® ND-1000 spectrophotometer (Thermo Fisher Scientific Inc., Piscataway, NJ, USA). Specific DNA products were generated with an RT-PCR system (high-capacity cDNA Synthesis Kit; Applied Biosystems, Foster City, CA, USA). Primer used are described in Table 3 and expression of *Ephx2*, *Il-1β*, *Il-6*, and *Tnfα* was assessed by quantitative real-time PCR using SsoAdvanced™ Universal SYBR® Green Supermix (BioRad) and the Bio-Rad CFX96™ system. Relative abundance of target gene mRNA was measured using the ΔΔCT method with appropriate primers and normalized to Tata box-binding protein (*Tbp*) as previously described [34].

Statistical analyses

Data are expressed as means + standard error of the mean (SEM). All statistical analyses were performed with JMP program (SAS Institute Inc., Cary, NC, USA) using an unpaired heteroscedastic two-tail Student's *t* test. Differences were considered significant at $P \leq 0.05$ and highly significant at $P \leq 0.01$. Single symbol (such as *) corresponds to $P \leq 0.05$, while double (such as **) corresponds to $P \leq 0.01$.

Acknowledgements

We thank Dr S. Sing from the Hammock laboratory for TPPU. This work was supported by the National Institute of Health Grants (R01DK090492 and R01DK095359) to FGH. Research in the Bettaieb laboratory is supported by a grant from NIH (R00DK100736). Research in the Hammock laboratory is supported by (R01ES002710 and R01DK103616) and the Superfund Research Program from National Institute of Environmental Health Sciences (P42ES04699). Research in the Havel laboratory is supported by NIH grants (DK-095980, HL-107256, HL-121324) and a multicampus grant from the University of California Office of the President. Research in the Zeldin laboratory is funded by the Intramural Research Program of the NIH, National Institute of Environmental Health Sciences (Z01 ES025034 to DCZ). Drs Haj and Havel are key personnel and Co-Leaders of the Endocrinology and Metabolism Core of UC, Davis Mouse Metabolic Phenotyping Center (MMPC) which is funded by NIH/NIDDK grant U24DK092993.

Author contributions

AB and FGH participated in research design. AB, SK, YZ, HF, JG, SC, SB, and NH conducted experiments. PJH, AG, DCZ, and BDH contributed new reagents or analytic tools. AB and FGH performed data analysis. All authors were involved in writing and editing the manuscript and had final approval of the submitted and published version.

Conflict of interest

AB, BDH, DCZ, and FGH are coinventors on a patent held by the University of California on the use of soluble epoxide hydrolase inhibitors to treat diabetic nephropathy. BDH is a cofounder of EicOsis LLC that aims to move soluble epoxide hydrolase inhibitors to the clinic for the treatment of neuropathic and inflammatory pain.

References

1 Kellum JA (2015) Diagnostic criteria for acute kidney injury: present and future. *Crit Care Clin* **31**, 621–632.

2 Asanuma K & Mundel P (2003) The role of podocytes in glomerular pathobiology. *Clin Exp Nephrol* **7**, 255–259.

3 Komenda P, Rigatto C & Tangri N (2014) Estimated glomerular filtration rate and albuminuria: diagnosis, staging, and prognosis. *Curr Opin Nephrol Hypertens* **23**, 251–257.

4 Gill SS & Hammock BD (1980) Distribution and properties of a mammalian soluble epoxide hydrase. *Biochem Pharmacol* **29**, 389–395.

5 Yu Z, Xu F, Huse LM, Morisseau C, Draper AJ, Newman JW, Parker C, Graham L, Engler MM, Hammock BD *et al.* (2000) Soluble epoxide hydrolase regulates hydrolysis of vasoactive epoxyeicosatrienoic acids. *Circ Res* **87**, 992–998.

6 He J, Wang C, Zhu Y & Ai D (2016) Soluble epoxide hydrolase: a potential target for metabolic diseases. *J Diabetes* **8**, 305–313.

7 Imig JD, Zhao X, Zaharis CZ, Olearczyk JJ, Pollock DM, Newman JW, Kim IH, Watanabe T & Hammock BD (2005) An orally active epoxide hydrolase inhibitor lowers blood pressure and provides renal protection in salt-sensitive hypertension. *Hypertension* **46**, 975–981.

8 Olearczyk JJ, Quigley JE, Mitchell BC, Yamamoto T, Kim IH, Newman JW, Luria A, Hammock BD & Imig JD (2009) Administration of a substituted adamantyl urea inhibitor of soluble epoxide hydrolase protects the kidney from damage in hypertensive Goto-Kakizaki rats. *Clin Sci* **116**, 61–70.

9 Zhao X, Yamamoto T, Newman JW, Kim IH, Watanabe T, Hammock BD, Stewart J, Pollock JS, Pollock DM & Imig JD (2004) Soluble epoxide hydrolase inhibition protects the kidney from hypertension-induced damage. *J Am Soc Nephrol* **15**, 1244–1253.

10 Kim J, Yoon SP, Toews ML, Imig JD, Hwang SH, Hammock BD & Padanilam BJ (2015) Pharmacological inhibition of soluble epoxide hydrolase prevents renal interstitial fibrogenesis in obstructive nephropathy. *Am J Physiol Renal Physiol* **308**, F131–F139.

11 Manhiani M, Quigley JE, Knight SF, Tasoobshirazi S, Moore T, Brands MW, Hammock BD & Imig JD (2009) Soluble epoxide hydrolase gene deletion attenuates renal injury and inflammation with DOCA-salt hypertension. *Am J Physiol Renal Physiol* **297**, F740–F748.

12 Elmarakby AA, Faulkner J, Al-Shabrawey M, Wang MH, Maddipati KR & Imig JD (2011) Deletion of soluble epoxide hydrolase gene improves renal endothelial function and reduces renal inflammation and injury in streptozotocin-induced type 1 diabetes. *Am J Physiol Regul Integr Comp Physiol* **301**, R1307–R1317.

13 Chalasani N, Younossi Z, Lavine JE, Diehl AM, Brunt EM, Cusi K, Charlton M, Sanyal AJ, American Association for the Study of Liver Diseases, American College of Gastroenterology et al. (2012) The diagnosis and management of non-alcoholic fatty liver disease: practice guideline by the American Association for the Study of Liver Diseases, American College of Gastroenterology, and the American Gastroenterological Association. *Am J Gastroenterol* **107**, 811–826.

14 Welsh GI, Hale LJ, Eremina V, Jeansson M, Maezawa Y, Lennon R, Pons DA, Owen RJ, Satchell SC, Miles MJ *et al.* (2010) Insulin signaling to the glomerular podocyte is critical for normal kidney function. *Cell Metab* **12**, 329–340.

15 Cunningham PN, Wang Y, Guo R, He G & Quigg RJ (2004) Role of Toll-like receptor 4 in endotoxin-induced acute renal failure. *J Immunol* **172**, 2629–2635.

16 Takahashi K, Mizukami H, Kamata K, Inaba W, Kato N, Hibi C & Yagihashi S (2012) Amelioration of acute kidney injury in lipopolysaccharide-induced systemic inflammatory response syndrome by an aldose reductase inhibitor, fidarestat. *PLoS One* **7**, e30134.

17 Chen Y, Du Y, Li Y, Wang X, Gao P, Yang G, Fang Y, Meng Y & Zhao X (2015) Panaxadiol saponin and dexamethasone improve renal function in lipopolysaccharide-induced mouse model of acute kidney injury. *PLoS One* **10**, e0134653.

18 Li P, Guo Y, Bledsoe G, Yang ZR, Fan H, Chao L & Chao J (2015) Kallistatin treatment attenuates lethality and organ injury in mouse models of established sepsis. *Crit Care* **19**, 200.

19 Palermo M, Alves-Rosa F, Rubel C, Fernandez GC, Fernandez-Alonso G, Alberto F, Rivas M & Isturiz M

(2000) Pretreatment of mice with lipopolysaccharide (LPS) or IL-1beta exerts dose-dependent opposite effects on Shiga toxin-2 lethality. *Clin Exp Immunol* **119**, 77–83.
20 Gorriz JL & Martinez-Castelao A (2012) Proteinuria: detection and role in native renal disease progression. *Transplant Rev (Orlando)* **26**, 3–13.
21 Kato T, Mizuno S & Kamimoto M (2010) The decreases of nephrin and nuclear WT1 in podocytes may cause albuminuria during the experimental sepsis in mice. *Biomed Res* **31**, 363–369.
22 Schmidt C, Hocherl K, Schweda F, Kurtz A & Bucher M (2007) Regulation of renal sodium transporters during severe inflammation. *J Am Soc Nephrol* **18**, 1072–1083.
23 Liao J, Hwang SH, Li H, Liu JY, Hammock BD & Yang GY (2016) Inhibition of chronic pancreatitis and murine pancreatic intraepithelial neoplasia by a dual inhibitor of c-RAF and soluble epoxide hydrolase in LSL-KrasG12D/Pdx-1-Cre mice. *Anticancer Res* **36**, 27–37.
24 Hellweg CE, Arenz A, Bogner S, Schmitz C & Baumstark-Khan C (2006) Activation of nuclear factor kappa B by different agents: influence of culture conditions in a cell-based assay. *Ann N Y Acad Sci* **1091**, 191–204.
25 Chung CH, Fan J, Lee EY, Kang JS, Lee SJ, Pyagay PE, Khoury CC, Yeo TK, Khayat MF, Wang A *et al.* (2015) Effects of tumor necrosis factor-alpha on podocyte expression of monocyte chemoattractant protein-1 and in diabetic nephropathy. *Nephron Extra* **5**, 1–18.
26 Harris TR, Li N, Chiamvimonvat N & Hammock BD (2008) The potential of soluble epoxide hydrolase inhibition in the treatment of cardiac hypertrophy. *Congest Heart Fail* **14**, 219–224.
27 Ma FY, Liu J & Nikolic-Paterson DJ (2009) The role of stress-activated protein kinase signaling in renal pathophysiology. *Braz J Med Biol Res* **42**, 29–37.
28 Flanc RS, Ma FY, Tesch GH, Han Y, Atkins RC, Bennett BL, Friedman GC, Fan JH & Nikolic-Paterson DJ (2007) A pathogenic role for JNK signaling in experimental anti-GBM glomerulonephritis. *Kidney Int* **72**, 698–708.
29 Cao Y, Yang W, Tyler MA, Gao X, Duan C, Kim SO, Aronson JF, Popov V, Takahashi H, Saito H *et al.* (2013) Noggin attenuates cerulein-induced acute pancreatitis and impaired autophagy. *Pancreas* **42**, 301–307.
30 Chin BY, Mohsenin A, Li SX, Choi AM & Choi ME (2001) Stimulation of pro-alpha(1)(I) collagen by TGF-beta(1) in mesangial cells: role of the p38 MAPK pathway. *Am J Physiol Renal Physiol* **280**, F495–F504.
31 Lindenmeyer MT, Rastaldi MP, Ikehata M, Neusser MA, Kretzler M, Cohen CD & Schlondorff D (2008) Proteinuria and hyperglycemia induce endoplasmic reticulum stress. *J Am Soc Nephrol* **19**, 2225–2236.
32 Ohse T, Inagi R, Tanaka T, Ota T, Miyata T, Kojima I, Ingelfinger JR, Ogawa S, Fujita T & Nangaku M (2006) Albumin induces endoplasmic reticulum stress and apoptosis in renal proximal tubular cells. *Kidney Int* **70**, 1447–1455.
33 Harris TR, Bettaieb A, Kodani S, Dong H, Myers R, Chiamvimonvat N, Haj FG & Hammock BD (2015) Inhibition of soluble epoxide hydrolase attenuates hepatic fibrosis and endoplasmic reticulum stress induced by carbon tetrachloride in mice. *Toxicol Appl Pharmacol* **286**, 102–111.
34 Bettaieb A, Chahed S, Tabet G, Yang J, Morisseau C, Griffey S, Hammock BD & Haj FG (2014) Effects of soluble epoxide hydrolase deficiency on acute pancreatitis in mice. *PLoS One* **9**, e113019.
35 Bettaieb A, Chahed S, Bachaalany S, Griffey S, Hammock BD & Haj FG (2015) Soluble epoxide hydrolase pharmacological inhibition ameliorates experimental acute pancreatitis in mice. *Mol Pharmacol* **88**, 281–290.
36 Esposito V, Grosjean F, Tan J, Huang L, Zhu L, Chen J, Xiong H, Striker GE & Zheng F (2013) CHOP deficiency results in elevated lipopolysaccharide-induced inflammation and kidney injury. *Am J Physiol Renal Physiol* **304**, F440–F450.
37 Yang CC, Yao CA, Yang JC & Chien CT (2014) Sialic acid rescues repurified lipopolysaccharide-induced acute renal failure via inhibiting TLR4/PKC/gp91-mediated endoplasmic reticulum stress, apoptosis, autophagy, and pyroptosis signaling. *Toxicol Sci* **141**, 155–165.
38 Woo CW, Cui D, Arellano J, Dorweiler B, Harding H, Fitzgerald KA, Ron D & Tabas I (2009) Adaptive suppression of the ATF4-CHOP branch of the unfolded protein response by toll-like receptor signalling. *Nat Cell Biol* **11**, 1473–1480.
39 Reiser J, von Gersdorff G, Loos M, Oh J, Asanuma K, Giardino L, Rastaldi MP, Calvaresi N, Watanabe H, Schwarz K *et al.* (2004) Induction of B7-1 in podocytes is associated with nephrotic syndrome. *J Clin Invest* **113**, 1390–1397.
40 Saito T, Yamada E, Okada S, Shimoda Y, Tagaya Y, Hashimoto K, Satoh T, Mori M, Okada J, Pessin JE *et al.* (2014) Nucleobindin-2 is a positive regulator for insulin-stimulated glucose transporter 4 translocation in fenofibrate treated E11 podocytes. *Endocr J* **61**, 933–939.
41 Luo P, Zhou Y, Chang HH, Zhang J, Seki T, Wang CY, Inscho EW & Wang MH (2009) Glomerular 20-HETE, EETs, and TGF-beta1 in diabetic nephropathy. *Am J Physiol Renal Physiol* **296**, F556–F563.
42 Wang Q, Pang W, Cui Z, Shi J, Liu Y, Liu B, Zhou Y, Guan Y, Hammock BD, Wang Y *et al.* (2013) Upregulation of soluble epoxide hydrolase in proximal tubular cells mediated proteinuria-induced renal damage. *Am J Physiol Renal Physiol* **304**, F168–F176.

43 Liang Y, Jing Z, Deng H, Li Z, Zhuang Z, Wang S & Wang Y (2015) Soluble epoxide hydrolase inhibition ameliorates proteinuria-induced epithelial-mesenchymal transition by regulating the PI3K-Akt-GSK-3beta signaling pathway. *Biochem Biophys Res Comm* **463**, 70–75.
44 Lee CR, Imig JD, Edin ML, Foley J, DeGraff LM, Bradbury JA, Graves JP, Lih FB, Clark J, Myers P *et al.* (2010) Endothelial expression of human cytochrome P450 epoxygenases lowers blood pressure and attenuates hypertension-induced renal injury in mice. *FASEB J* **24**, 3770–3781.
45 Kim J, Imig JD, Yang J, Hammock BD & Padanilam BJ (2014) Inhibition of soluble epoxide hydrolase prevents renal interstitial fibrosis and inflammation. *Am J Physiol Renal Physiol* **307**, F971–F980.
46 Singh A, Gudehithlu KP, Le G, Litbarg NO, Khalili V, Vernik J, Hart P, Arruda JA & Dunea G (2004) Decreased urinary peptide excretion in patients with renal disease. *Am J Kidney Dis* **44**, 1031–1038.
47 Waldmann TA, Strober W & Mogielnicki RP (1972) The renal handling of low molecular weight proteins. II. Disorders of serum protein catabolism in patients with tubular proteinuria, the nephrotic syndrome, or uremia. *J Clin Invest* **51**, 2162–2174.
48 Harrison JF, Lunt GS, Scott P & Blainey JD (1968) Urinary lysozyme, ribonuclease, and low-molecular-weight protein in renal disease. *Lancet* **1**, 371–375.
49 Harrison JF & Blainey JD (1967) Low molecular weight proteinuria in chronic renal disease. *Clin Sci* **33**, 381–390.
50 Creeth JM, Kekwick RA, Flynn FV, Harris H & Robson EB (1963) An ultracentrifuge study of urine proteins with particular reference to the proteinuria of renal tubular disorders. *Clin Chim Acta* **8**, 406–414.
51 Butler EA, Flynn FV, Harris H & Robson EB (1962) A study of urine proteins by two-dimensional electrophoresis with special reference to the proteinuria of renal tubular disorders. *Clin Chim Acta* **7**, 34–41.
52 Butler EA & Flynn FV (1958) The proteinuria of renal tubular disorders. *Lancet* **2**, 978–980.
53 Lorenzen J, Shah R, Biser A, Staicu SA, Niranjan T, Garcia AM, Gruenwald A, Thomas DB, Shatat IF, Supe K *et al.* (2008) The role of osteopontin in the development of albuminuria. *J Am Soc Nephrol* **19**, 884–890.
54 Guzman J, Jauregui AN, Merscher-Gomez S, Maiguel D, Muresan C, Mitrofanova A, Diez-Sampedro A, Szust J, Yoo TH, Villarreal R *et al.* (2014) Podocyte-specific GLUT4-deficient mice have fewer and larger podocytes and are protected from diabetic nephropathy. *Diabetes* **63**, 701–714.
55 Dickson LE, Wagner MC, Sandoval RM & Molitoris BA (2014) The proximal tubule and albuminuria: really!. *J Am Soc Nephrol* **25**, 443–453.
56 Tenten V, Menzel S, Kunter U, Sicking EM, van Roeyen CR, Sanden SK, Kaldenbach M, Boor P, Fuss A, Uhlig S *et al.* (2013) Albumin is recycled from the primary urine by tubular transcytosis. *J Am Soc Nephrol* **24**, 1966–1980.
57 Liu D, Wen Y, Tang TT, Lv LL, Tang RN, Liu H, Ma KL, Crowley SD & Liu BC (2015) Megalin/cubulin-lysosome-mediated albumin reabsorption is involved in the tubular cell activation of NLRP3 inflammasome and tubulointerstitial inflammation. *J Biol Chem* **290**, 18018–18028.
58 Verma R, Venkatareddy M, Kalinowski A, Patel SR, Salant DJ & Garg P (2015) Shp2 associates with and enhances nephrin tyrosine phosphorylation and is necessary for foot process spreading in mouse models of podocyte injury. *Mol Cell Biol* **36**, 596–614.
59 Guijarro C & Egido J (2001) Transcription factor-kappa B (NF-kappa B) and renal disease. *Kidney Int* **59**, 415–424.
60 Massy ZA, Guijarro C, O'Donnell MP, Kim Y, Kashtan CE, Egido J, Kasiske BL & Keane WF (1999) The central role of nuclear factor-kappa B in mesangial cell activation. *Kidney Int Suppl* **71**, S76–S79.
61 Lan Y, Zhou Q & Wu ZL (2004) NF-kappa B involved in transcription enhancement of TGF-beta 1 induced by Ox-LDL in rat mesangial cells. *Chin Med J* **117**, 225–230.
62 El Karoui K, Viau A, Dellis O, Bagattin A, Nguyen C, Baron W, Burtin M, Broueilh M, Heidet L, Mollet G *et al.* (2016) Endoplasmic reticulum stress drives proteinuria-induced kidney lesions via lipocalin 2. *Nat Commun* **7**, 10330.
63 Yu L, Liu Y, Wu Y, Liu Q, Feng J, Gu X, Xiong Y, Fan Q & Ye J (2014) Smad3/Nox4-mediated mitochondrial dysfunction plays a crucial role in puromycin aminonucleoside-induced podocyte damage. *Cell Signal* **26**, 2979–2991.
64 Cybulsky AV (2013) The intersecting roles of endoplasmic reticulum stress, ubiquitin- proteasome system, and autophagy in the pathogenesis of proteinuric kidney disease. *Kidney Int* **84**, 25–33.
65 Cybulsky AV (2010) Endoplasmic reticulum stress in proteinuric kidney disease. *Kidney Int* **77**, 187–193.
66 Chiang CK, Hsu SP, Wu CT, Huang JW, Cheng HT, Chang YW, Hung KY, Wu KD & Liu SH (2011) Endoplasmic reticulum stress implicated in the development of renal fibrosis. *Mol Med* **17**, 1295–1305.
67 Li SS, Ye JM, Deng ZY, Yu LX, Gu XX & Liu QF (2015) Ginsenoside-Rg1 inhibits endoplasmic reticulum stress-induced apoptosis after unilateral ureteral obstruction in rats. *Ren Fail* **37**, 890–895.
68 Schley G, Klanke B, Schodel J, Forstreuter F, Shukla D, Kurtz A, Amann K, Wiesener MS, Rosen S, Eckardt KU *et al.* (2011) Hypoxia-inducible transcription factors stabilization in the thick ascending

limb protects against ischemic acute kidney injury. *J Am Soc Nephrol* **22**, 2004–2015.
69 Heyman SN, Brezis M, Epstein FH, Spokes K, Silva P & Rosen S (1991) Early renal medullary hypoxic injury from radiocontrast and indomethacin. *Kidney Int* **40**, 632–642.
70 Burlington H & Cronkite EP (1973) Characteristics of cell cultures derived from renal glomeruli. *Proc Soc Exp Biol Med* **142**, 143–149.
71 Krakower CA & Greenspon SA (1954) Factors leading to variation in concentration of nephrotoxic antigen(s) of glomerular basement membrane. *AMA Arch Pathol* **58**, 401–432.
72 Ren Q, Ma M, Ishima T, Morisseau C, Yang J, Wagner KM, Zhang JC, Yang C, Yao W, Dong C *et al*. (2016) Gene deficiency and pharmacological inhibition of soluble epoxide hydrolase confers resilience to repeated social defeat stress. *Proc Natl Acad Sci USA* **113**, E1944–E1952.
73 Lee KS, Liu JY, Wagner KM, Pakhomova S, Dong H, Morisseau C, Fu SH, Yang J, Wang P, Ulu A *et al*. (2014) Optimized inhibitors of soluble epoxide hydrolase improve in vitro target residence time and in vivo efficacy. *J Med Chem* **57**, 7016–7030.
74 Haj FG, Zabolotny JM, Kim YB, Kahn BB & Neel BG (2005) Liver-specific protein-tyrosine phosphatase 1B (PTP1B) re-expression alters glucose homeostasis of PTP1B-/-mice. *J Biol Chem* **280**, 15038–15046.